Intestinal Delivery Profiles of 2-mm Nutrient Microbeads ("Microtransporters"): In-Vitro Release Integrated with Physiological Gastric Transport

Daniel Reither[1], Alexander Gruber[1], Michael Huttegger[1], Daniel Wallerstorfer[1]

[1]Laboratory, Novogenia GmbH, Salzburg, Austria

Corresponding Author: Daniel Wallerstorfer (ceo@novogenia.com)

ABSTRACT

Background:
The stomach regulates the transfer of ingested material into the duodenum according to its physical form and energy density. Low-energy liquids are emptied rapidly, whereas small digestible solids empty more slowly and large indigestible particles are typically retained until interdigestive clearance by the migrating motor complex (MMC) (Goyal et al., 2019; Abell et al., 2008; Li et al., 2022). Particle size plays a decisive role, as studies show that solids up to roughly 3 mm can pass post-prandially, whereas larger ones remain until phase III contractions (Stotzer et al., 2000; Leiper et al., 1993). These physiological differences in gastric sieving and motility are fundamental determinants of nutrient delivery timing and intestinal availability (Maurer et al., 2015).

Methods:
Two spherical 2-mm vitamin C loaded microbeads — one fast-release and one slow-release — were characterized in an isothermal intestinal buffer while release was tracked continuously via pH and converted to percent release with a calibration curve. In addition, a mixed-release composition containing equal proportions of fast- and slow-release beads (50:50) was evaluated to model intermediate release behavior representative of blended formulations. To map in vitro curves to realistic post-ingestion timelines, literature-based gastric emptying functions for liquids versus small solids were parameterized and superimposed on the dissolution profiles (Goyal et al., 2019; Abell et al., 2008; Mudie et al., 2014; Li et al., 2022; Maurer et al., 2015).

Results:
In intestinal buffer, the fast-release beads liberated about 70% of their payload within the first 10 min and reached nearly complete release by 60 min, consistent with rapid diffusion through a permeable matrix under sink conditions. The slow-release beads showed a more gradual, diffusion-controlled profile, reaching full release only after ~3 h with a near-linear mid-phase. This contrast mirrors classical sustained-release behavior observed in biorelevant media (Klein, 2010; Leigh et al., 2013). When these in-vitro data

were convolved with physiological gastric transport functions, the resulting timelines diverged sharply; solutes from the fast-release beads, which follow the rapid emptying of gastric liquids, entered the small intestine within ~1.5 h after ingestion. Acid-resistant slow-release beads, behaving as small solids (<3 mm), emptied more slowly and began releasing only upon entering the duodenum, creating an extended intestinal delivery window of ~7 h. A mixed-release composition (50% fast and 50% slow release) produced an intermediate profile, maintaining continuous nutrient release throughout the 7-hour period and effectively bridging the gap between the rapid and sustained formats. This slower transit is consistent with human observations that small indigestible particles clear over 3–4 h, while larger ones are retained until an interdigestive phase III contraction (Stotzer et al., 2000; Leiper et al., 1993).

Discussion:
These findings illustrate how controlled-release microbeads can either front-load absorption opportunities, as in the fast-release design, or distribute nutrient exposure over several hours, as in the slow-release configuration. The mixed-release formulation further demonstrated that combining fast- and slow-release components can yield a continuous, steady release profile, providing a more balanced and extended nutrient availability across the full intestinal transit period. The contrasting kinetics leverage established physiological differences between liquid and small-solid gastric handling and the inherent variability of small-bowel transit (Goyal et al., 2019; Abell et al., 2008; Maurer et al., 2015; Stotzer et al., 2000; Leiper et al., 1993). Together, these results highlight how coupling in-vitro release data with validated gastric emptying parameters provides a physiologically grounded framework for predicting when and where nutrients become bioaccessible in the intestine.

Subjects: Gastrointestinal Transit Modeling **Keywords:** Gastric emptying, Microbeads, Nutrient Delivery, Physiological Modeling

INTRODUCTION

The human stomach meters the delivery of ingested material into the duodenum according to physical form and caloric density. Water and other low-energy liquids empty rapidly; digestible solids empty more slowly and often after an initial lag while particles are mechanically reduced; large indigestible particles tend to be retained until the interdigestive migrating motor complex (MMC) clears them, although small indigestible particles of roughly 2–3 mm may pass post-prandially under certain conditions (Stotzer et al., 2000; Leiper et al., 1993). These principles are well established by scintigraphic, manometric, and magnetic resonance studies and are summarized in recent reviews and consensus statements (Goyal et al., 2019; Abell et.al, 2008).

Controlled-release multiparticulates — millimeter-scale beads, pellets, or granules — have long been used in pharmaceutics to decouple release from gastric residence and to spread exposure across intestinal segments. For nutrient delivery, the same logic can be applied: an uncoated, highly permeable bead is expected to dissolve rapidly; an acid-resistant, diffusion-controlled bead is expected to delay and smooth release so that a smaller fraction of payload appears in the early duodenum and more appears distally. However, in vitro dissolution curves alone do not reveal when after ingestion a nutrient becomes available in the small intestine; the answer depends on how quickly liquids or small solids traverse the stomach. The present work therefore characterizes release in a simple intestinal buffer and then maps those curves onto evidence-based gastric emptying functions for liquids versus small solids to obtain delivery profiles that are anchored in human physiology (Goyal et al., 2019; Abell et.al, 2008; Li et al., 2022).

METHODS

Overview

The investigation was conducted in three interconnected stages: (1) the characterization and parameterization of stomach-to-intestine transport kinetics for liquids and small solids based on published physiological data; (2) the experimental quantification of vitamin C release from 2-mm microbeads under controlled intestinal buffer conditions; and (3) the mathematical superimposition of the physiological transport functions with the in-vitro release curves to generate post-ingestion nutrient delivery timelines that reflect realistic gastrointestinal behavior.

Section 1 – Physiological Stomach-to-Intestine Transport

A narrative evidence synthesis was conducted to parameterize the gastric emptying behavior of (a) liquids and dissolved solutes and (b) digestible small solids. For liquids, rapid emptying was described using a first-order function with a half-time of approximately 10–20 min, consistent with direct measurements of gastric water clearance ($T_{50} \approx 13 \pm 1$ min) and previous reports showing that low-energy liquids are typically emptied from the stomach within the first hour (Mudie et al., 2014; Goyal et al., 2019; Abell et al., 2008).

For digestible small solids, a sigmoidal emptying function with a brief lag phase followed by a slower evacuation over roughly 2–4 h was applied, reflecting the well-established distinction between solid and liquid gastric kinetics and the selective retention of larger particles until they are sufficiently reduced and homogenized with chyme.

Figure 1. Modeled Gastric Retention of Liquids and Digestible Small Solids (<3 mm) Based on Goyal et al. (2019).

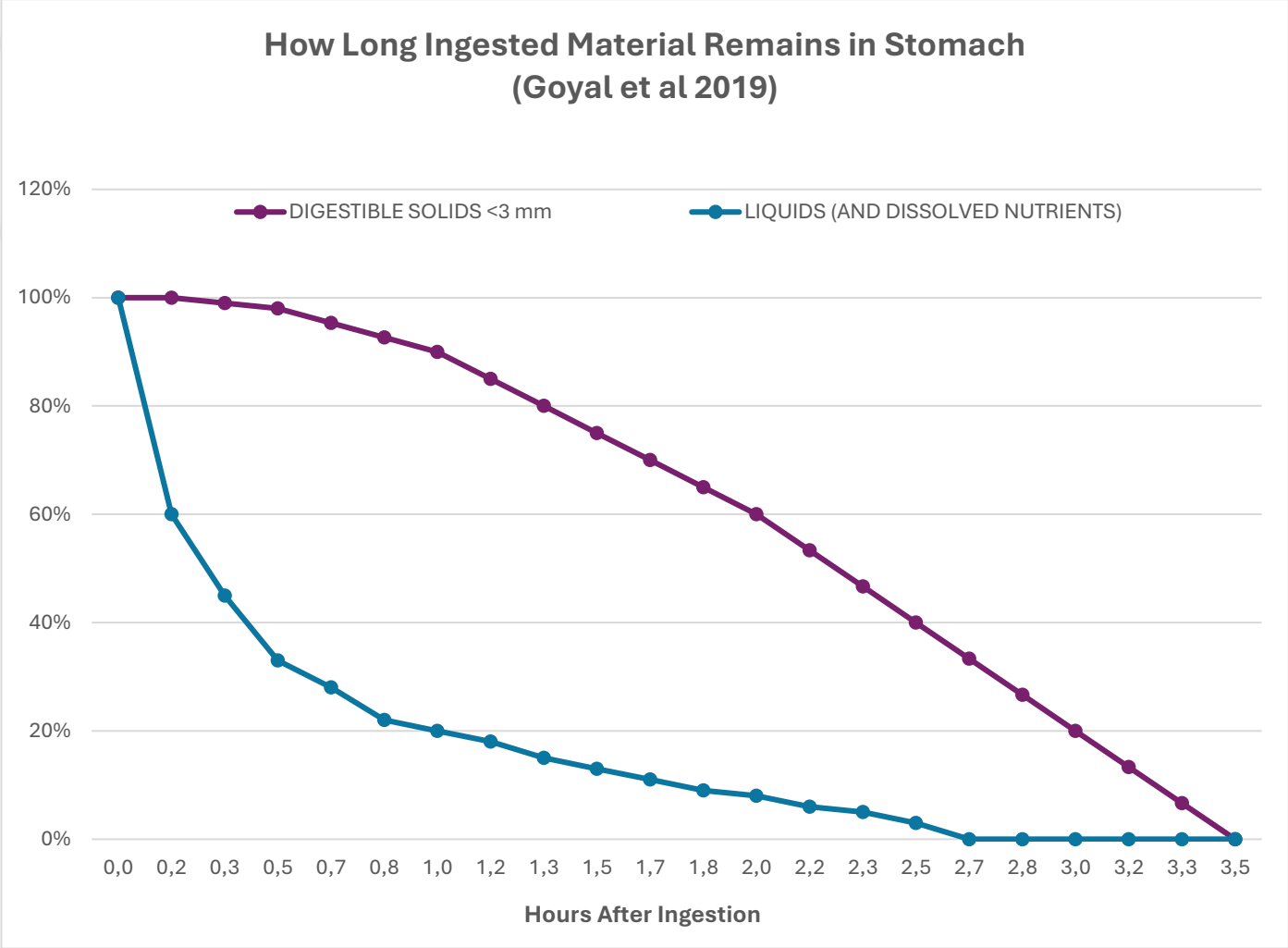

Percentage of material remaining in the stomach versus time (0–3.5 h) for liquids and digestible small solids (<3 mm) based on Goyal et al. (2019). Liquids (and dissolved nutrients) empty rapidly, with ~70 % transferred to the small intestine within the first hour. Digestible small solids empty more gradually, reaching complete transfer after approximately 3–3.5 h.

The special case of indigestible particulates was also considered. Large, non-deformable particles (>5–7 mm) are typically retained in the stomach during the fed period and are only cleared during phase III of the MMC; by contrast, particles at or below a few millimeters can empty post-prandially under certain physiological conditions. Human scintigraphic and manometric studies have shown that particles up to ~3, and in some cases even slightly larger, may pass through the pylorus without requiring an interdigestive phase III event (Stotzer et al., 2000; Leiper et al., 1993). These observations

justify modeling 2-mm microbeads as digestible small solids that empty more slowly than liquids but do not depend on interdigestive clearance (Goyal et al., 2019; Li et al., 2022).

The resulting transport functions were normalized to 100% transfer to the small intestine by ~3.5 h for liquids and ~3–4 h for small solids, consistent with typical human gastric emptying physiology while allowing for interindividual variability in transit times.

Section 2 – In-Vitro Intestinal Release: Vitamin C Model

Two bead formats were fabricated at a 2.0-mm nominal diameter to ensure comparable surface area-to-volume ratios between formulations. The fast-release format consisted of a water-permeable polymeric matrix without an acid-resistant barrier, allowing immediate hydration and diffusion of the vitamin C payload once exposed to aqueous conditions. In contrast, the slow-release format incorporated an acid-resistant exterior designed to suppress gastric dissolution, combined with a diffusion- and erosion-controlling sublayer to prolong release in the intestinal environment.

Release testing was conducted in a sodium phosphate intestinal buffer maintained at 37 °C under gentle stirring to simulate physiological mixing. The release of vitamin C was monitored continuously by tracking the pH decrease associated with ascorbic acid ionization. The pH signal was subsequently converted to percentage released using a calibration curve obtained by titrating known quantities of crystalline vitamin C into the same buffer and fitting ΔpH to concentration. Replicate dissolution vessels produced smooth cumulative release profiles over 0–8 h, and incremental 10-min release rates were calculated by differencing consecutive cumulative data points to capture short-term release kinetics with high temporal resolution.

RESULTS

Section 2 – In-Vitro Intestinal Release

The fast-release microbeads exhibited an immediate burst phase, with approximately 70% of the encapsulated vitamin C released within the first 10 min and nearly complete release (≈100%) achieved by 60 min. This rapid liberation reflects the unrestricted diffusion of the soluble payload through the water-permeable matrix once hydrated under sink conditions. In contrast, the slow-release beads demonstrated a more gradual, diffusion-controlled profile characterized by a shallow initial burst followed by a steadily increasing release rate, reaching approximately 100% after about 3 h. The extended mid-phase of the curve indicates sustained diffusion through the internal polymer network and progressive erosion of the rate-controlling sublayer. These behaviors are consistent with the intended functional design of the two systems—the permeable matrix promoting rapid diffusion in the fast-release format, and the acid-resistant, diffusion-barrier architecture providing prolonged release in the slow-release formulation.

Figure 2. Cumulative Nutrient Release in Intestinal Buffer (In-Vitro Conditions).

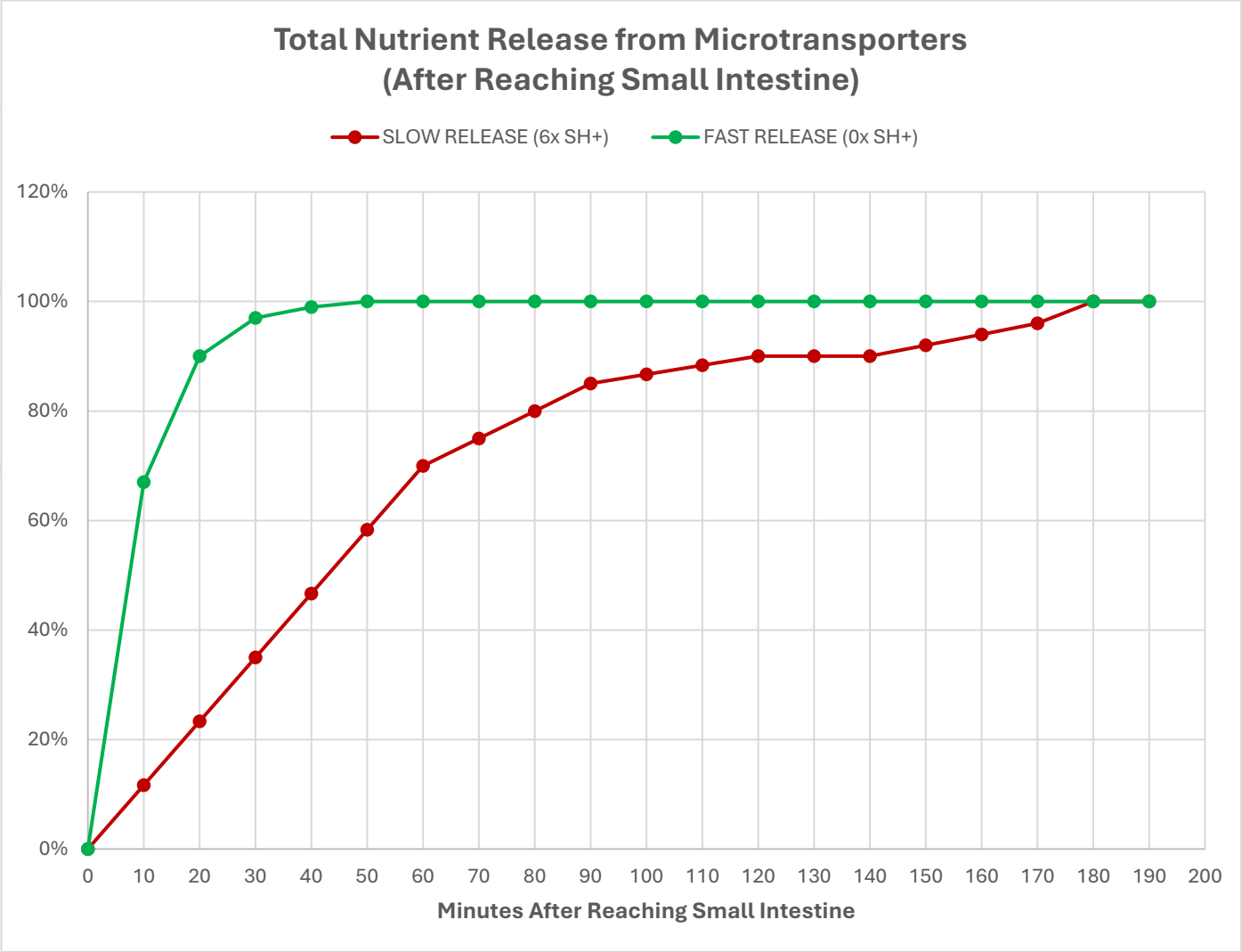

Cumulative percent release versus time (0–8 h) for fast- and slow-release beads in intestinal buffer at 37 °C. The fast-release curve rises steeply to 100% by 1 h; the slow-release curve rises gradually to 100% by ~3 h.

Figure 3. Incremental Nutrient Release per 10-Minute Interval in Intestinal Buffer.

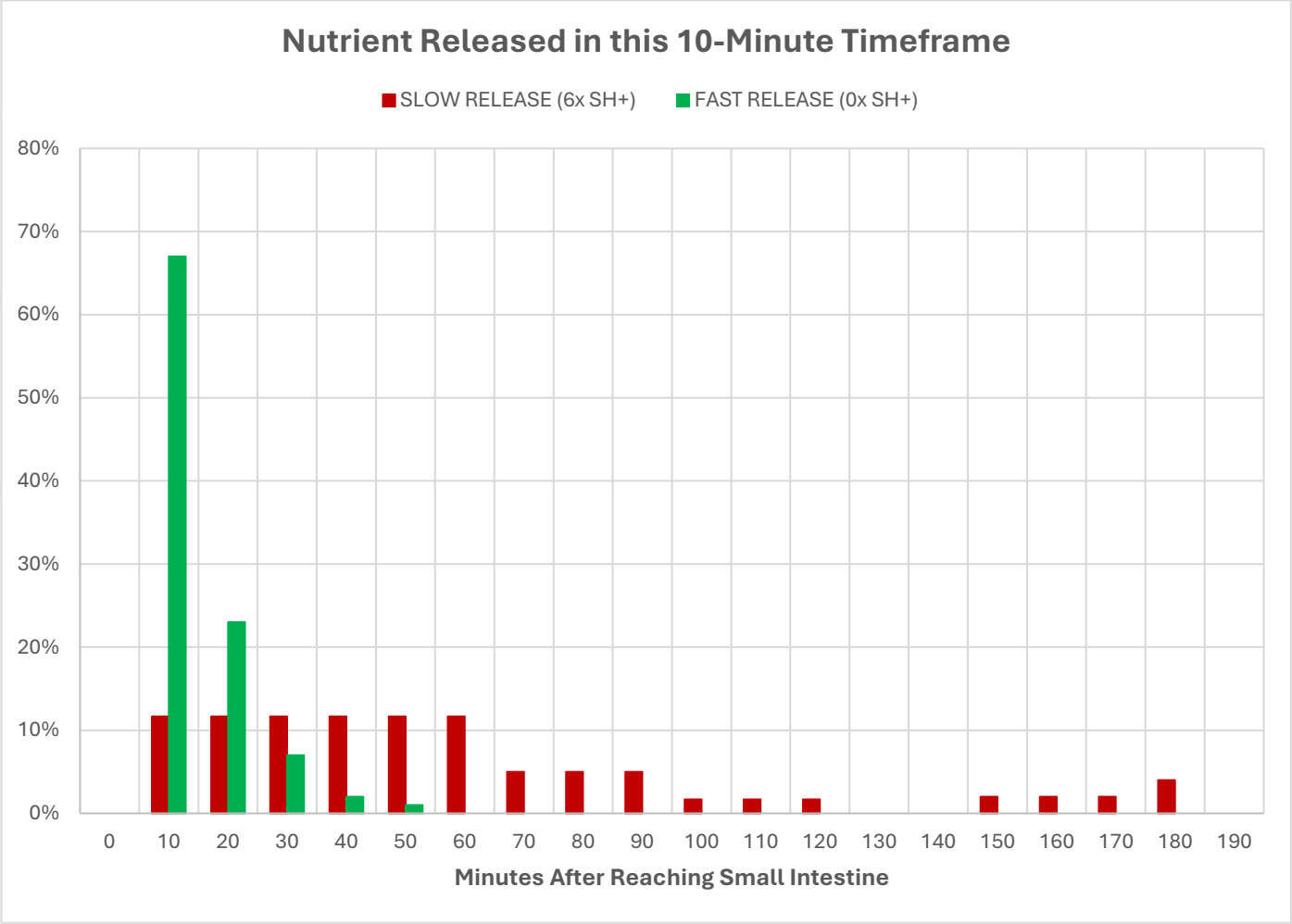

Percent released within each 10-minute bin. The fast-release format shows a narrow, high spike within the first 30–40 min; the slow-release format shows a broader, lower plateau peaking between ~2.5 and 3.5 h.

Section 3 – Post-Ingestion Delivery Following Superimposed Gastric Transport

When the in-vitro release curves were superimposed onto the modeled gastric transport functions, the resulting simulations revealed two distinct physiological pathways that produced markedly different windows of intestinal absorption opportunity.

For the fast-release format, the nutrient was liberated rapidly into the gastric fluid, becoming part of the liquid phase and subsequently transported to the duodenum with the rapid emptying characteristic of water and other low-energy fluids. Consequently, the majority of absorbable vitamin C reached the small intestine within approximately 1.5 h of ingestion, producing a front-loaded exposure profile dominated by the first post-ingestive hour. This predicted behavior aligns closely with measured half-times for gastric water emptying (T_{50} ≈ 13 min) and with the well-documented precedence of liquid over solid emptying dynamics in human physiology (Mudie et al., 2014; Abell et al., 2008).

In contrast, the slow-release formulation remained intact during gastric residence due to its acid-resistant exterior, behaving physiologically as a small solid. The combination

of slower gastric emptying and the intrinsic ~3 h diffusion-controlled release observed in intestinal buffer resulted in a prolonged nutrient delivery window extending to approximately 7 h after ingestion. The broad, low-amplitude release profile implies a reduced likelihood of competition at intestinal transport sites and may promote nutrient uptake along more distal small-bowel segments. The classification of the 2-mm beads as small solids is consistent with human motility data, which demonstrate that post-prandial emptying of particles around 2–3 mm can occur without requiring interdigestive clearance, whereas substantially larger indigestible particles are typically retained until phase III of the migrating motor complex (Goyal et al., 2019; Li et al., 2022; Stotzer et al., 2000).

To further explore intermediate release behavior, a mixed formulation containing equal proportions of the fast- and slow-release beads (50:50) was modeled. The resulting mixed-release profile exhibited a continuous, extended release pattern spanning the full 7 h period, bridging the gap between the rapid initial availability of the fast-release formulation and the prolonged delivery of the slow-release system. This combination produced a smoother and more sustained nutrient supply curve, representing a potential strategy for achieving balanced, long-term intestinal exposure across physiological transit conditions.

Figure 4. Cumulative Nutrient Released to the Intestinal Lumen After Ingestion (Physiology-Informed Timeline).

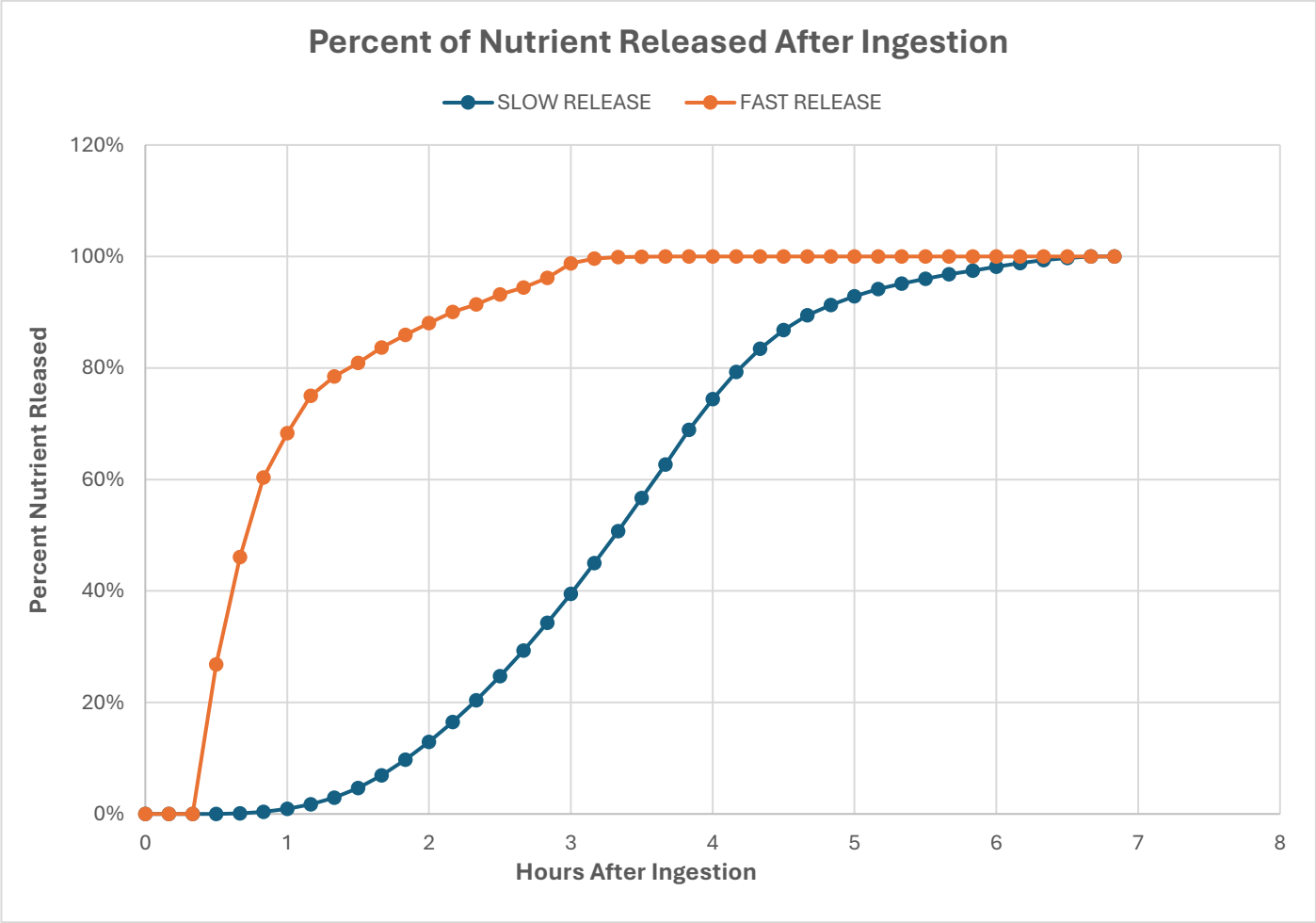

Cumulative percent released versus time after ingestion, obtained by convolving gastric transport with in-vitro release. The fast-release curve reaches ~100% by ~1.5–2 h; the slow-release curve climbs steadily and approaches 100% around ~7 h.

Figure 5. Incremental Nutrient Release per 10-Minute Interval After Ingestion (Physiology-Informed Timeline).

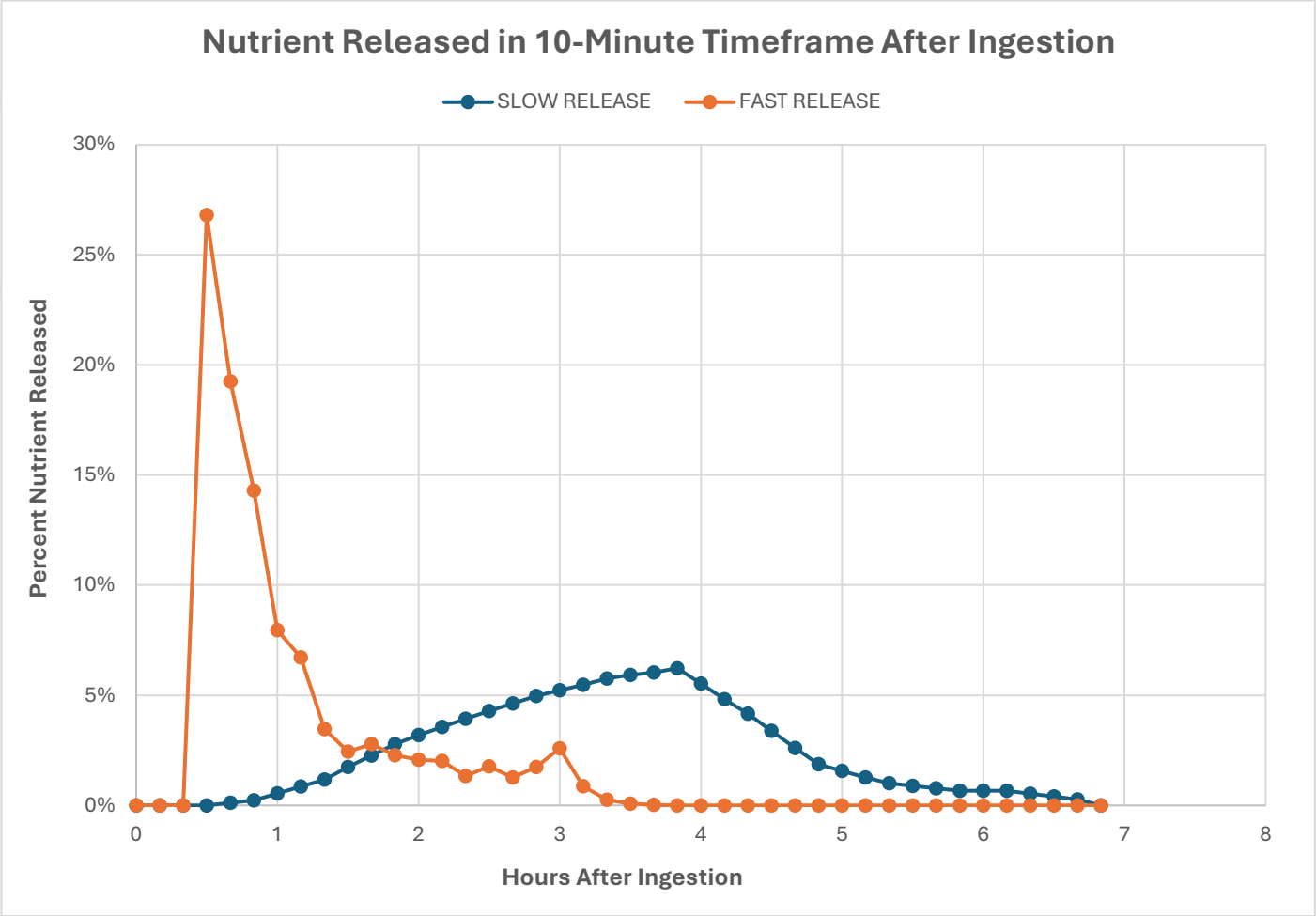

Percent released in each 10-minute bin after ingestion. The fast-release format exhibits a sharp early peak within the first hour; the slow-release format shows a flattened, sustained distribution extending several hours.

Figure 6. Cumulative Nutrient Released to the Intestinal Lumen After Ingestion (Physiology-Informed Timeline) for slow and fast mixed.

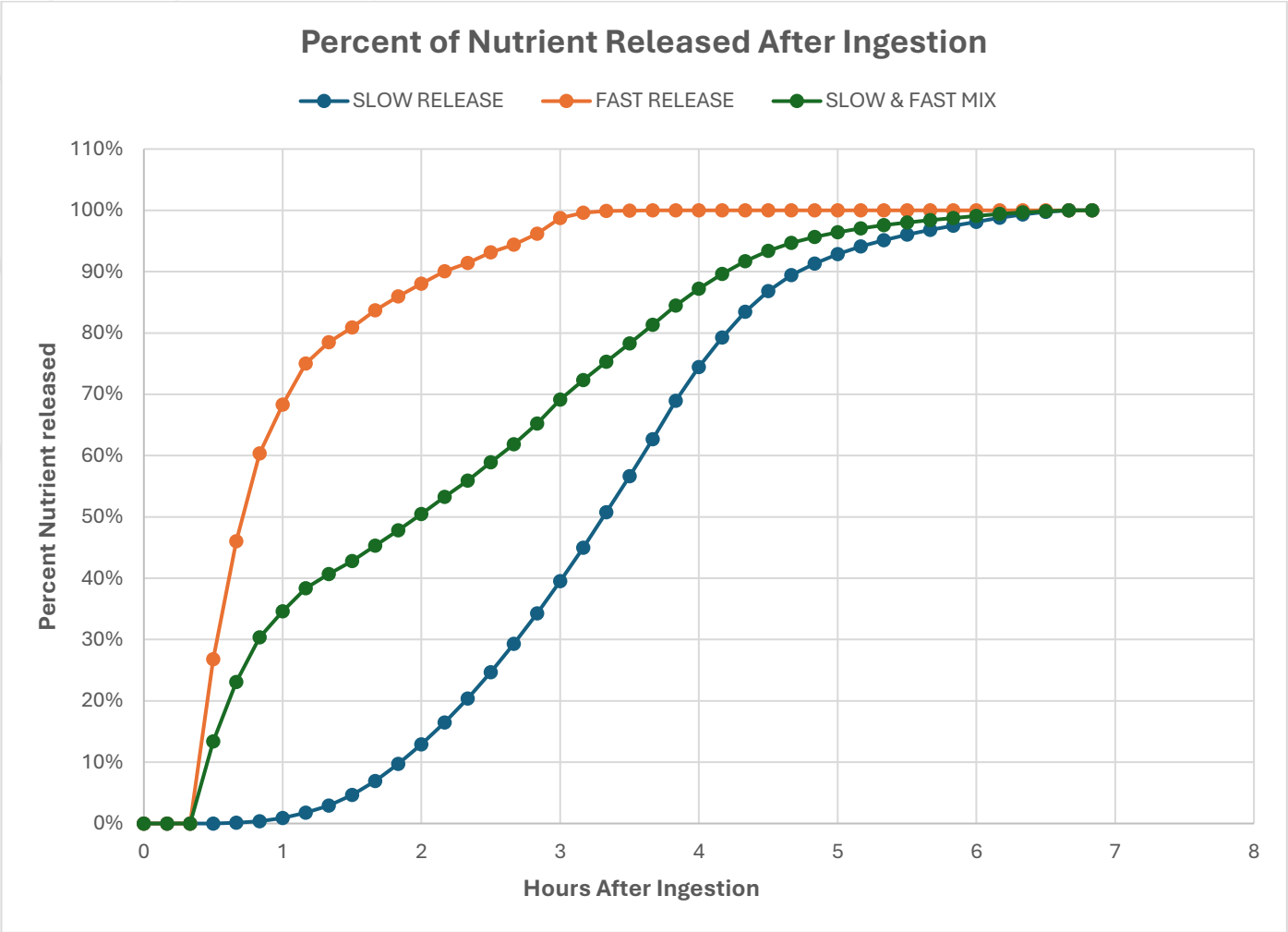

Cumulative percent of nutrient released versus time (0–8 h) after ingestion, modeled by convolving in-vitro release data with physiological gastric transport. The fast-release formulation shows a steep rise, reaching nearly 100% release within ~1.5 h. The slow-release formulation exhibits a gradual, diffusion-controlled profile approaching complete release by ~7 h. The combined formulation (50% fast and 50% slow) produces an intermediate curve, reflecting the additive behavior of both fast and slow release phases and yielding a broadened nutrient-delivery window.

Figure 7. Incremental Nutrient Release per 10-Minute Interval for Fast-, Slow-, and Mixed-Release Formats (Physiology-Informed Timeline).

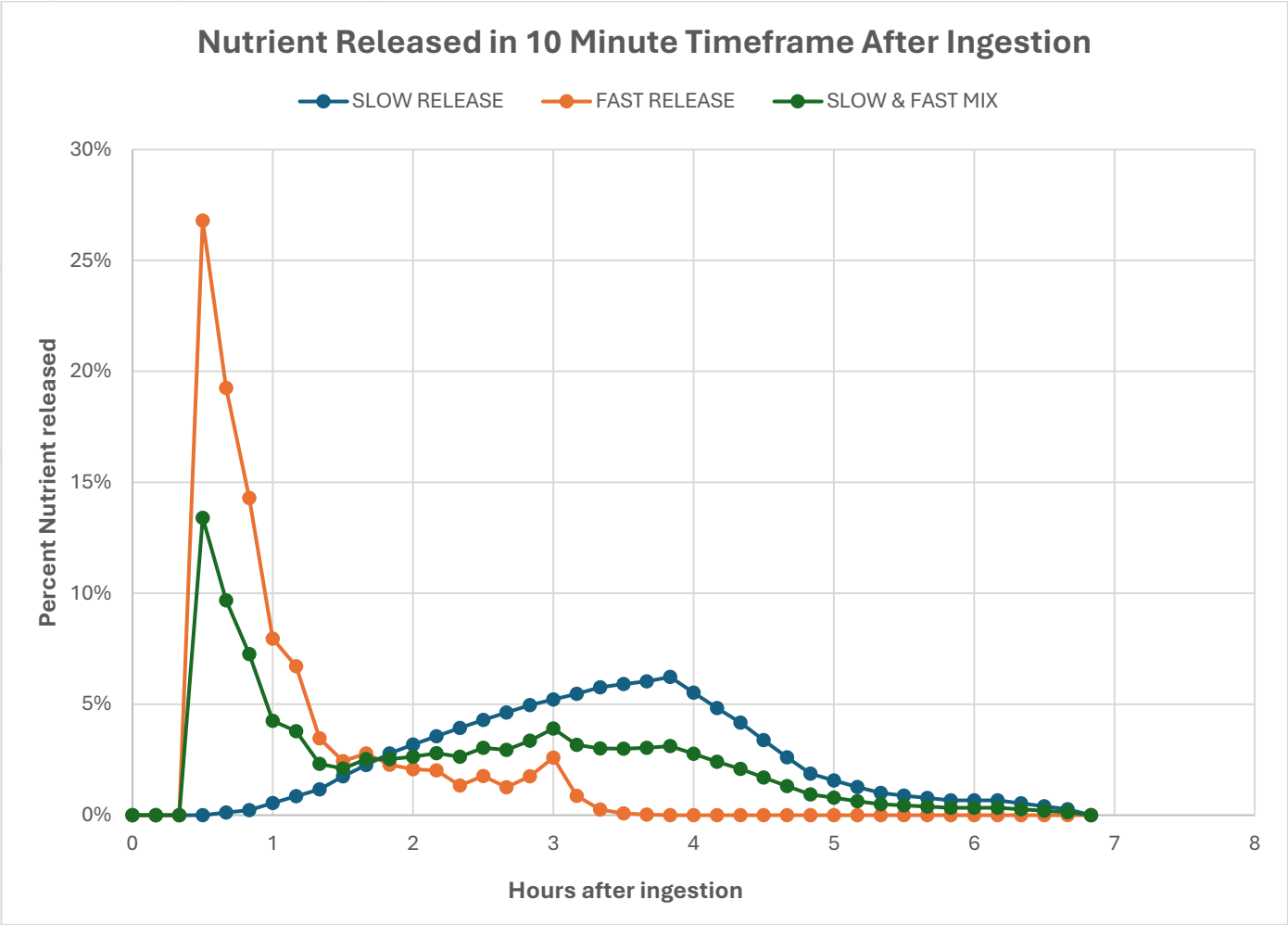

Percent of nutrients released in each 10-minute interval after ingestion. The fast-release format shows a sharp, early peak within the first hour, reflecting rapid gastric emptying and immediate diffusion. The slow-release format displays a broader, lower-amplitude profile that extends over several hours, indicating sustained release. The mixed-release composition (50% fast and 50% slow) produces an intermediate pattern with a continuous, moderately elevated release rate throughout the 7-hour period, illustrating a balanced combination of rapid and prolonged nutrient delivery.

DISCUSSION

Mapping dissolution profiles onto gastric transport transforms in-vitro release data into physiologically interpretable nutrient delivery timelines. The fast-release format generates a concentrated, early exposure profile suited to actives that benefit from rapid appearance in the proximal small intestine or synchronization with food intake. In contrast, the slow-release format produces prolonged, lower-amplitude exposure that may reduce competition at intestinal transporters and mitigate oxidation-mediated interactions among co-administered nutrients. From a physiological perspective, this contrast reflects two sequential mechanisms: (1) selective gastric sieving, in which liquids empty rapidly while digestible small solids are retained longer, and (2) matrix-controlled diffusion and erosion once the beads enter the intestinal lumen (Goyal et al., 2019; Abell et al., 2008).

Building on these two distinct release behaviors, a mixed formulation containing equal proportions of fast- and slow-release beads was modeled to simulate intermediate nutrient delivery dynamics. The resulting mixed-release profile produced a continuous, steady release pattern spanning approximately seven hours, bridging the gap between the rapid initial availability of the fast-release formulation and the sustained output of the slow-release system. This mixed configuration demonstrates how combining microbeads with different release kinetics can achieve a more uniform nutrient supply across the entire intestinal transit period, potentially enhancing bioavailability and mimicking the gradual nutrient absorption seen with natural food digestion.

Several nuances merit consideration. First, liquid emptying is strongly influenced by energy density; the presence of carbohydrates, proteins, or fat slows gastric outflow relative to plain water. The current liquid-phase assumption is therefore most accurate for low-energy gastric contents and should be adjusted upward when co-ingestion involves caloric beverages (Goyal et al., 2019).

Second, particle-size thresholds for post-prandial emptying are not absolute. Although traditional models emphasize retention of particles >2 mm until the interdigestive phase, human motility studies have demonstrated that solids up to approximately 3 mm — and occasionally larger — can pass during the fed state, depending on meal composition, antral motility, and particle deformability (Goyal et al., 2019; Li et al., 2022; Stotzer et al., 2000; Leiper et al., 1993).

Third, small-bowel transit adds further dispersion, as typical transit times range over several hours with considerable interindividual variability, implying that distal intestinal segments may contribute significantly to uptake during prolonged release (Maurer et al., 2015).

Finally, the pH-tracking approach used for vitamin C offers a continuous, low-noise proxy for release dynamics because ascorbic acid donates protons and induces predictable shifts in buffer pH. The calibration curve generated in the same medium enables direct conversion of ΔpH into concentration, avoiding sampling artifacts and providing high-resolution release-rate data. For non-acidic actives, the same framework can be implemented using UV/visible spectrophotometry or LC–MS quantification while preserving the transport-superposition methodology.

Limitations

The intestinal buffer employed in this study represents a simplified medium compared with more physiologically relevant systems such as FaSSIF-V2 (pH ≈ 6.5; containing bile salts and phospholipids), which more accurately replicate the composition and micellar solubilization capacity of the fasted-state small intestine. Nevertheless, the superposition framework applied here is inherently agnostic to the dissolution medium. Future investigations could readily substitute the buffer-based release curves with data obtained in FaSSIF or FeSSIF media without altering the underlying transport modeling or physiological interpretation (Leigh et al., 2013; Klein, 2010).

Furthermore, gastric emptying behavior is known to vary with factors such as meal size, macronutrient composition, and individual physiological differences. The transfer functions used in this model therefore reflect average population kinetics rather than

patient-specific parameters. To establish clinical relevance, subsequent studies should include segmental sampling or pharmacokinetic validation to confirm that the modeled delivery timelines accurately reflect in-vivo nutrient appearance and absorption dynamics (Abell et al., 2008; Maurer, 2015).

CONCLUSION

Fast- and slow-release 2-mm nutrient microbeads exhibit fundamentally different post-ingestion availability windows when realistic gastric transport dynamics are considered. The fast-release format produces a front-loaded intestinal availability profile, with most of the nutrient becoming accessible within approximately 90 minutes after ingestion, reflecting rapid gastric emptying and immediate diffusion from the permeable matrix. In contrast, the slow-release format achieves a prolonged and gradual delivery phase, extending nutrient availability over nearly seven hours as a result of the combined effects of slower gastric evacuation of small solids and diffusion-controlled intestinal release. This divergence highlights the influence of both formulation architecture and gastrointestinal physiology on nutrient exposure kinetics.

In addition to these two distinct release modes, a mixed-release formulation composed of equal proportions of fast- and slow-release beads demonstrated an intermediate and continuous release pattern spanning the full 7-hour period. This balanced profile offers the advantages of both formats — rapid initial delivery followed by sustained release — potentially providing a more consistent nutrient supply across the intestinal transit time and a closer approximation to physiological absorption patterns observed with complex foods.

The integrated modeling approach combines in-vitro release measurements with physiology-based gastric transport simulation through convolution and offers a transparent, reproducible, and mechanistically grounded framework for the rational design and optimization of nutrient delivery systems. It enables researchers to predict intestinal exposure profiles from laboratory data more accurately, improving the translational understanding of how formulation properties interact with physiological transport processes.

Author contributions, funding, and data availability

Microbead design, fabrication, and testing were performed within the developer's laboratory. Data curation, modeling, and manuscript drafting were completed by the same team. Funding was provided by the organization that manufactures the microtransporters; relevant intellectual property may be held by the authors or their affiliates. Release time-series, calibration curves, and superposition code will be made available with the submitted manuscript.

REFERENCES

- Abell TL, Camilleri M, Donohoe K, et al. Consensus recommendations for gastric emptying scintigraphy: a joint report of the American Neurogastroenterology and Motility Society and the Society of Nuclear Medicine. *J Nucl Med Technol.* 2008;36(1):44-54.
- Goyal RK, Guo Y, Mashimo H. Advances in the physiology of gastric emptying. *Neurogastroenterol Motil.* 2019;31(4):e13546.
- Mudie DM, Murray K, Hoad CL, et al. Quantification of gastrointestinal liquid volumes and distribution following a 240 mL dose of water in the fasted state. *Mol Pharm.* 2014;11(9):3039-3047.
- Li Y, Owyang C, Shi X, et al. Simulating human gastrointestinal motility in dynamic in-vitro systems. *Compr Rev Food Sci Food Saf.* 2022;21(5):
- Maurer AH. Gastrointestinal motility, Part 2: small-bowel and colon transit. *J Nucl Med.* 2015;56(9):1395-1400.
- Leigh M, Kloefer B, Schaich M. Comparison of the solubility and dissolution of drugs in fasted-state biorelevant media (FaSSIF and FaSSIF-V2). *Dissolution Technol.* 2013;20(3):44-51.
- Klein S. The use of biorelevant dissolution media to forecast the in vivo performance of a drug. *AAPS J.* 2010;12(3):397-406.
- Stotzer PO, Abrahamsson H. Human postprandial gastric emptying of indigestible solids can occur unrelated to antral phase III. *Neurogastroenterol Motil.* 2000;12(6): [pagination not verified]; doi:10.1046/j.1365-2982.2000.00218.x.